

# Numerical simulations of a reduced model for blood coagulation

Jevgenija Pavlova, Antonio Fasano and Adélia Sequeira

**Abstract.** In this work the three-dimensional numerical resolution of a complex mathematical model for the blood coagulation process is presented. The model was illustrated in [18, 36]. It incorporates the action of the biochemical and cellular components of blood as well as the effects of the flow. The model is characterized by a reduction of the biochemical network and considers the impact of the blood slip at the vessel wall. The numerical results showing the capacity of the model to predict different perturbations in the hemostatic system are discussed.

**Mathematics Subject Classification (2010).** Primary 92C10, 92C45; Secondary 76M10.

**Keywords.** Blood coagulation, cell-based model, platelets, fibrin, blood slip velocity, reaction-advection-diffusion equations.

## 1. Introduction

The ability of the body to control blood flow in the presence of a vascular injury is crucial for survival. Blood coagulation is an extremely complex biological process that is responsible for the formation of clots, preventing bleeding. An equally complex mechanism is set in motion to gradually dissolve clots, followed by the repair of the injured tissue. These processes involve complex interactions between multiple molecular and cellular components in the blood and vessel wall, and it is also influenced by the flow of blood [9, 19, 35, 38, 42, 43, 44, 47].

It is very important that coagulation takes place only when necessary and is stopped before the clot becomes an obstacle to blood flow. Thus it requires a fine triggering mechanism, followed by a very efficient positive feedback effect and by a likewise effective brake. This is achieved by a strict balance among the so called coagulation factors, their inhibitors, and the fibrinolytic reagents that control the clot evolution and allow the blood to flow without any major obstacles.

All these processes go through many steps and if they fail at some stage various disorders can be caused [7, 14, 17] which can be extremely dangerous. Such disorders belong to two main groups: bleeding<sup>1</sup> and obstructive thrombosis<sup>2</sup> disorders according to whether coagulation is hindered, with consequent hemorrhagic phenomena or accelerated leading to pathological thrombi formation [22, 47]. According to [16] every year only in Europe more than a half million of people die due to coagulation disorders. This number is even higher than the total number of deaths caused by AIDS, breast cancer, prostate cancer and road traffic accidents combined together<sup>3</sup>.

---

<sup>1</sup>Bleeding disorders were known in the antiquity, particularly in connection with circumcision. The first bleeding disorder—von Willebrand disease—was reported in 1920s; later, in 1930s scientists recognized the role of platelets-free plasma, that served as the beginning of the discovering of the coagulation factors that appeared later in 1960s. Source: [www.hemophilia.org](http://www.hemophilia.org)

<sup>2</sup>Already in 1856 the German pathologist Rudolph Virchow published the pathophysiology of pulmonary embolism and identified its possible source in what later became known as the Virchow's triad.

<sup>3</sup>Source [www.thrombosisadviser.com](http://www.thrombosisadviser.com).

In order to prevent the consequences of blood coagulation related diseases it is crucial to understand the dynamics of clot formation, growth and dissolution. Numerous laboratory tests are done to identify the components (both cellular and molecular) and the mechanical properties of blood clots<sup>4</sup>. The main anticoagulant drugs are heparin, greatly enhancing the action of antithrombin ATIII, Plavix, acting on platelets, Warfarin that prevents the vitamin K formation in the liver, etc. Also the anticoagulant properties of aspirin are well known. Research on new anticoagulants is in full development. Drugs like apixaban, rivaroxaban, etc. are based on a different principles and seem to be very effective [32]. Nowadays biology and biochemistry are more and more closely connected to mathematics and computations associated to mathematical models. Different mathematical models for blood coagulation can be found e.g. in [1, 2, 3, 4, 5, 6, 11, 19, 20, 21, 29, 31, 48]. Numerical tests provide new ideas and help to build new biological hypothesis that can be first tested numerically, saving the time and need for laboratory tests.

Hereby, we consider the mathematical model for platelets-fibrin clot formation introduced in [18] and partially validated in [36], where the impact of the slip velocity was shown (see also [37]). In the model, the chain of biochemical reactions was reduced replacing ten reactions describing the initial and amplification phases of a cell-based blood coagulation model by only one virtual equation for prothrombinase production. An important feature was the introduction of a blood slip velocity possibly leading to an accumulation of activated platelets at the clotting region promoting a higher thrombin production<sup>5</sup>. This extra platelet supply at the clotting site may help explaining different clot structures according to the local blood dynamics. Therefore the model had the advantage of incorporating some novelty, at the same time proposing a substantial reduction of the differential system describing the chemical cascade.

Though the results of [18], in the context of some artificial geometry, were encouraging, only a full three dimensional can be considered a reasonable validity test. This is precisely the scope of the present work.

The outline of the paper is as follows. In Section 1 the mathematical model is summarized; in Section 2 the numerical techniques to solve the blood coagulation problem are explained; in Section 3 the numerical results in three-dimensional case and capacity of the model to predict some disorder cases are discussed.

## 2. Mathematical model

The mathematical model below combines the biochemistry of blood coagulation with the mechanical properties of the blood flow, taking the model of [6] as a benchmark in a simplified geometrical context. It consists of a nonlinear system of 13 reaction-advection-diffusion (RAD) partial differential equations—describing a network of biochemical reactions—coupled with a generalized Newtonian fluid

---

<sup>4</sup>Pharmaceutical companies have provided a number of vital drugs that have extended the life expectancy of patients, such as a QuikClot<sup>®</sup> that helps to accelerate the coagulation process in case of external bleeding that was developed by US Naval Medical Research Institute in 2008. Moreover, scientists are working on a generation of synthetic platelets, based on Arg-Gly-Asp functionalized nanoparticles, that are more resistant to transportation than the donor platelets [10]. Also recently UK researchers developed a new technique to synthesize red blood cells (RBC) from stem cells (Marc Turner is the principal researcher in this project that is funded by the Wellcome Trust). These RBC are now of appropriate quality and standards and they may be safely transmitted into humans.

<sup>5</sup>The information sources on thrombin generation can be found in [13, 33, 34].

with shear-thinning viscosity function—to model the blood flow.

$$\begin{cases} \rho(\mathbf{u}_t + \mathbf{u} \cdot \nabla \mathbf{u}) = \operatorname{div} \sigma(\mathbf{u}, p), & \text{in } \Omega, \\ \operatorname{div} \mathbf{u} = 0, & \text{in } \Omega, \\ \mathbf{n}^T \sigma(\mathbf{u}, p) \mathbf{n} = \alpha \mathbf{n} \cdot \mathbf{u} = 0, & \text{on } \partial\Omega_{slip}, \\ \mathbf{n}^T \sigma(\mathbf{u}, p) \boldsymbol{\tau} = \beta \mathbf{u} \cdot \boldsymbol{\tau}, & \text{on } \partial\Omega_{slip}, \\ \sigma(\mathbf{u}, p) \mathbf{n} = 0, & \text{on } \partial\Omega_{out}, \\ \mathbf{u}(\mathbf{x}, t) = \mathbf{u}^*, & \text{on } \partial\Omega_{in}, \\ \mathbf{u}(\mathbf{x}, 0) = \mathbf{u}^0, & \text{on } \Omega, \end{cases} \quad (1)$$

$$\begin{cases} (C_i)_t + \operatorname{div}(C_i \mathbf{u}) - \operatorname{div}(D_i \nabla C_i) = R_i, & \text{in } \Omega, \\ -\mathbf{u} C_i \cdot \mathbf{n} = 0, & \text{on } \partial\Omega_{slip} \cup \partial\Omega_{out}, \\ C_i(\mathbf{x}, t) = C_i^{blood}, & \text{on } \partial\Omega_{in}, \\ C_i(\mathbf{x}, 0) = C_i^0, & \text{on } \Omega. \end{cases} \quad (2)$$

Here,  $(\mathbf{u}, p)$  stands for the blood velocity vector field and scalar function pressure,  $\sigma(\mathbf{u}, p)$  is the stress tensor defined by

$$\sigma(\mathbf{u}, p) = 2\mu(\dot{\gamma}) \mathbf{D}(\mathbf{u}) - p\mathbf{I},$$

where the function  $\mu(\dot{\gamma})$  is the viscosity function depending on the shear rate;  $\mathbf{n}$  and  $\boldsymbol{\tau} = (\tau_1, \tau_2)$  are the normal, tangential and bi-tangential vectors to the blood vessel boundary  $\partial\Omega = \partial\Omega_{in} \cup \partial\Omega_{out} \cup \partial\Omega_{slip}$ , where  $\partial\Omega_{in}$  and  $\partial\Omega_{out}$  correspond to the inflow and outflow boundaries and  $\partial\Omega_{slip}$  corresponds to the blood vessel walls;  $\mathbf{u}^0$  is the initial condition for the velocity field and  $\mathbf{u}^*$  is the entrance velocity that represent a trace of the initial velocity at the inlet surface;  $C_i(\mathbf{x}, t)$ ,  $i = 1, \dots, 13$  are scalar functions representing the time evolution of the concentration of each coagulation or fibrinolytic factor in the space domain  $\Omega$ ;  $R_i$  are nonlinear terms describing the chain of chemical reactions;  $D_i$  are the diffusion coefficients;  $C_i^{blood}$  are the inflow boundary conditions and  $C_i^0$  are the initial conditions for each coagulation factor  $i$ —we assume that a small blood clot has been already formed during the initial and amplification phases.

The reaction terms  $R_i$  are listed below

$$R_W = k_W \hat{C}_P [IIa] \left( 1 - \frac{[IIa]}{[IIa]^*} \right) - (h_{1W}[APC] + h_{2W}[ATIII])[W], \quad (3)$$

$$R_{IIa} = \frac{k_2[W][II]}{K_{2M} + [II]} - h_2[IIa][ATIII], \quad (4)$$

$$R_{II} = -\frac{k_2[W][II]}{K_{2M} + [II]}, \quad (5)$$

$$R_{Ia} = \frac{k_1[IIa][I]}{K_{1M} + [I]} - \frac{h_1[PLA][Ia]}{H_{1M} + [Ia]}, \quad (6)$$

$$R_I = -\frac{k_1[IIa][I]}{K_{1M} + [I]}, \quad (7)$$

$$R_{ATIII} = -h_2[IIa][ATIII] - h_{2W}[W][ATIII], \quad (8)$$

$$R_{APC} = \frac{k_{PC}[IIa][PC]}{K_{PCM} + [PC]} - h_{PC}[APC][\alpha_1 AT] - h_{1W}[APC][W], \quad (9)$$

$$R_{PC} = -\frac{k_{PC}[IIa][PC]}{K_{PCM} + [PC]}, \quad (10)$$

TABLE 1. The values used in (16) to update the platelets concentration.

Parameters	Values
$A_P$	$\min\left(\frac{V_n}{V_n^*}, 1\right)$
$V_n$	0.001 cm/min
$V_n^*$	0.00025 cm/min
$h$	0.001cm
$H$	$\frac{\pi R_{core}^3}{2}$ cm
$[Ia]^*$	350 nM

$$R_{\alpha_1 AT} = -h_{PC}[APC][\alpha_1 AT], \quad (11)$$

$$R_{tPA} = 0, \quad (12)$$

$$R_{PLA} = \frac{k_{PLA}[tPA][PLS]}{K_{PLAM} + [PLS]} - h_{PLA}[PLA][\alpha_2 AP], \quad (13)$$

$$R_{PLS} = -\frac{k_{PLA}[tPA][PLS]}{K_{PLAM} + [PLS]}, \quad (14)$$

$$R_{\alpha_2 AP} = -h_{PLA}[PLA][\alpha_2 AP]. \quad (15)$$

In these equations  $[\cdot]$  denotes the concentration of the corresponding coagulation factors. We stress that (3) does not describe real reactions, but rather a virtual process summarizing a whole set of reactions regulating the production of prothrombinase and involving many more coagulation factors<sup>6</sup>. In this respect  $[W]$  need not represent the actual prothrombinase concentration, but should be interpreted as an auxiliary function, as it was pointed out in [18], leading to the correct determination of the thrombin and fibrin. The reaction and inhibition rates  $k_{\square}$  and  $h_{\square}$  are taken from [6, 36]. The parameter  $\hat{C}_P$  in (3) stands for the dimensionless platelets concentration and in its simplest form (see [18]) is given by

$$\hat{C}_P = \left(1 + \frac{1}{2} \frac{A_P}{V_n} \frac{h}{H} u_s \frac{[Ia]}{[Ia]^*} \frac{u}{u_s}\right). \quad (16)$$

Here, the factor  $\frac{1}{2}$  stands as an assumption that the slip velocity occurs mainly upstream the clot;  $A_P$  is the fraction of incoming activated platelets;  $V_n$  is the blood clot normal velocity;  $h$  is the thickness of a slipping layer above the clot carrying activated platelets<sup>7</sup>;  $H$  is an aspect ratio dependent on the injury shape and its orientation towards the blood flow<sup>8</sup> and  $u_s$  is the blood slip velocity;  $[Ia]^*$  is the fibrin threshold concentration defining the clot boundary<sup>9</sup>, see Table 1.

In our simulations the domain  $\Omega = \{(x_1, x_2, x_3) \in \mathbb{R}^3 : (x_1^2 + x_2^2) \leq r, 0 < x_3 < l\}$  represents an idealized blood vessel with radius  $r = 250\mu\text{m}$  and length  $l = 1500\mu\text{m}$ .

The parameters  $\alpha$  and  $\beta$  in (1)<sub>3,4</sub> are chosen in such a way that the blood velocity along the vessel walls is equal to 5% of the imposed maximum velocity  $U_{max} = 8$  cm/s and in the normal direction satisfies the no-penetration condition:  $\alpha = 10^{24}$  and  $\beta = 40$ .

Initial conditions for the velocity field  $\mathbf{u}^0$  are obtained by solving the stationary Stokes problem with slip boundary conditions and initial clot inside the computational domain  $\Omega$ , since the process is started from the propagation phase assuming that the injury is covered by an initial blood clot.

The blood clot is modeled in terms of the fibrin concentration saying that it is formed in those vessel regions where fibrin concentration has achieved a threshold value that we set equal to 350 nM

<sup>6</sup>We recall that if one has to study disorders related with the deficiency or dysfunction of any of the bypassed factors, then it is clear that the shortcut represented by (3) is no longer admissible.

<sup>7</sup>The thickness of the slipping layer is estimated to be of the order of ten platelets diameter, see [18].

<sup>8</sup>For a circular shape of radius  $R$  we have  $H = \frac{\pi}{2}R$ .

<sup>9</sup>More details about the model, the virtual equation and possible extensions may be found in [18, 36, 37].

[46]. Moreover, the clot region is identified by the domain  $\Omega_{clot}$  that is fully included into the blood vessel domain  $\Omega$  and is given as  $\Omega_{clot} = \Omega_{core} + \Omega_{layer}$ , where  $\Omega_{core}$  is the core region and  $\Omega_{layer}$  the slipping layer. The core region completely covers the injury site and for simplicity both these domains are taken as parts of ellipsoids  $E_1$  and  $E_2$  centered at the center point of the injury  $(x_1^*, x_2^*, x_3^*) \in \partial\Omega$  with radii  $R_{core}^{(m)}$  and  $R_{layer}^{(m)}$ , respectively, where the index  $m = 1, 2, 3$  prescribes the height, width and length of the initial clot

$$\Omega_{core} = \{(x_1, x_2, x_3) : \Omega \cap E_1; E_1 := \frac{(x_1 - x_1^*)^2}{(R_{core}^{(1)})^2} + \frac{(x_2 - x_2^*)^2}{(R_{core}^{(2)})^2} + \frac{(x_3 - x_3^*)^2}{(R_{core}^{(3)})^2} < 1\},$$

$$\Omega_{layer} = \{(x_1, x_2, x_3) : \Omega \cap E_2 \setminus E_1; E_2 := \frac{(x_1 - x_1^*)^2}{(R_{layer}^{(1)})^2} + \frac{(x_2 - x_2^*)^2}{(R_{layer}^{(2)})^2} + \frac{(x_3 - x_3^*)^2}{(R_{layer}^{(3)})^2} < 1\}.$$

Moreover, we assume that fresh blood doesn't contain any of the activated coagulation factors entering (3)–(15), therefore, the non-zero concentration of activated coagulation factors is present practically only inside and downstream the clot (due to convection, diffusion has little influence). On the contrary, non-active coagulation factors are present in their maximum amount in the fresh blood, while inside the clot their concentration drops significantly.

Accordingly, the initial concentrations within the whole computational domain can be defined by the following functions

$$C_i^{active}(t_{PP}, \mathbf{x}) = f_i^{(1)}(\mathbf{x}) \quad \text{and} \quad C_j^{non-active}(t_{PP}, \mathbf{x}) = f_j^{(2)}(\mathbf{x}).$$

Here, index  $i$  stands for the active coagulation factors: prothrombinase (W), thrombin (factor IIa), fibrin (factor Ia), active protein C (APC) and plasmin (PLA); index  $j$  stands for the non-active coagulation factors: prothombin (factor II), fibrinogen (factor I), protein C (PC), alpha-1 antitrypsin( $\alpha_1$ AT), tissue plasminogen activator (tPA), plasminogen (PLS) and alpha 2-antiplasmin( $\alpha_2$ AP); time  $t_{PP}$  stands for the beginning of the propagation phase (PP) and functions  $f_i^{(1)}(\mathbf{x})$  and  $f_j^{(2)}(\mathbf{x})$  are defined by

$$f_i^{(1)}(\mathbf{x}) = \begin{cases} C_i^0, & \text{in } \Omega_{core} \\ C_i^{blood}, & \text{in } \Omega \setminus \Omega_{core} \cup \Omega_{layer}, \\ -C_i^0 \cdot T_1, & \text{in } \Omega_{layer} \end{cases}$$

and

$$f_j^{(2)}(\mathbf{x}) = \begin{cases} C_j^0, & \text{in } \Omega_{core} \\ C_j^{blood}, & \text{in } \Omega \setminus \Omega_{core} \cup \Omega_{layer}. \\ C_j^{blood} \cdot T_2 - C_j^0 \cdot T_1, & \text{in } \Omega_{layer} \end{cases}$$

Here  $C_i^0$  and  $C_j^0$  are the initial concentrations of active and non-active coagulation factors taken at the end of the amplification phase;  $C_i^{blood}$  and  $C_j^{blood}$ [36] are the concentrations of coagulation factors in the fresh blood [6], see Table 2; functions  $T_1$  and  $T_2$  are defined by

$$T_1 = -\frac{1 - X_1}{X_1 - X_2}, \quad T_2 = \frac{1 - X_2}{X_1 - X_2},$$

with  $X_1$  and  $X_2$  defined by

$$X_k = \frac{(x_1 - x_1^*)^2}{(R_k^{(1)})^2} + \frac{(x_2 - x_2^*)^2}{(R_k^{(2)})^2} + \frac{(x_3 - x_3^*)^2}{(R_k^{(3)})^2}, \quad k = 1, 2,$$

where  $(x_1^*, x_2^*, x_3^*)$  is the center point of the injury, as already mentioned.

TABLE 2. Concentration of coagulation factors inside the initial blood clot and fresh blood [6, 36].

Coagulation factors	Initial clot concentration (nM)	Fresh blood concentration (nM)
W	1.0843	0.0
II	1195.8306	1400.0
IIa	0.6865	0.0
I	6654.5100	7000.0
Ia	350.1488	0.0
PC	59.8972	60.0
APC	0.1588	0.0
ATIII	1566.1334	3400.0
$\alpha_1$ AT	44999.8284	45000.0
PLS	2178.26097	2180.0
PLA	3.8671	0.0
$\alpha_2$ AP	104.9480	105.0
tPA	0.0906	0.08

### 3. Numerical resolution

For the numerical solution of the blood coagulation model we used the Finite Element Method (FEM). The numerical implementation is done using an open source finite element solver FreeFem++<sup>10</sup> and the mesh is built taking an advantage of an automatic FreeFem++ mesh generator based on the Delaunay-Voronoi algorithm, Fig. 1. In our simulations a fixed mesh is used, that is refined in the clot region and contains 23.862 degrees of freedom (DoFs)<sup>11</sup>.

The blood flow and biochemical problems are solved sequentially, but the linear systems coming from the space and time discretizations are solved in parallel using the sparse direct MULTifunctional Massively Parralel (MUMPS) solver<sup>12</sup>. The direct method implemented in MUMPS is based on a multi-frontal approach and to solve the system it constructs a direct factorization  $A = LU$ ,  $A = L^TDL$  depending on the symmetry of the matrix  $A$ .

The computation time required to simulate the blood coagulation process using the synthetic model in the two- and the three-dimensional cases is shown in Table 3. We expect that a larger number of processors will decrease the computational time, however, that is not necessarily the case. It can happen that a greater number of processors will increase the computational time and decrease the quality of the convergence due to the amount of communications between the machines.

The outline of the model resolution is the following: solve the blood flow problem (1); update the platelets concentration (16); solve the biochemical problem (2).

In the next sections the numerical methods to solve the blood and biochemical problems are presented.

<sup>10</sup>FreeFem++ is a powerful tool that is suitable for the resolution of 2D and 3D multiphysics problems [23]. It has its own high level programming language based on C++; it provides an access to different direct and iterative solvers and, moreover, it gives an access to the parallel solvers (using the parallel version MPI [12, 27, 39, 40]) that are extremely important in our case moving to the resolution of the three-dimensional problem.

<sup>11</sup>This number increases up to 1.431.720 DoFs adopting the mesh to the blood coagulation problem with 13 unknowns in the biochemical problem approximated with P1 elements and 4 unknowns for the blood flow problem approximated with P1 and P2 elements.

<sup>12</sup>It is possible to apply the Domain Decomposition Method, or other techniques and solve the bigger part of the problem in parallel.

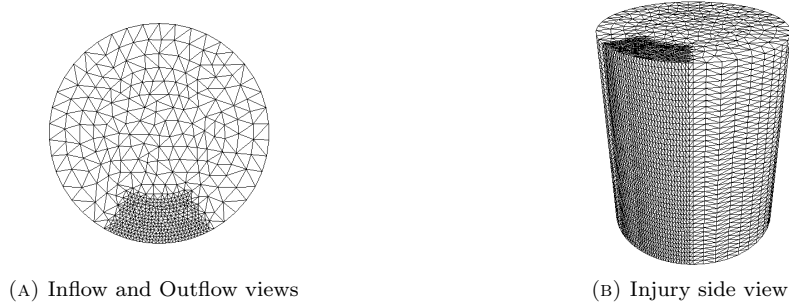


FIGURE 1. Three-dimensional computational domain.

TABLE 3. Computational cost to simulate 60 seconds of the blood coagulation process.

Computational domain			Computational time (hours)	Number of processors
2D	Number of triangles	6320	1.75	1
	Number of vertices	3274		
3D	Number of tetrahedrals	131040	6	4
	Number of vertices	23862	5	8
			4.5	12
			4.3	24

### 3.1. Fluid subproblem

In this section we recall the numerical resolution of the blood flow problem by presenting the variational formulation of problem (1) and its discretization in space by the finite element method. The nonlinear convective term is linearized using a semi-implicit scheme while the time advance is performed using an implicit Euler method.

We introduce the following spaces for the velocity and pressure test functions

$$V := \{\mathbf{v} \in (H^1(\Omega))^d : \mathbf{v}|_{\partial\Omega} = \mathbf{g}\}, \text{ and } Q := L^2(\Omega) = \{q \in L^2(\Omega) : \int_{\Omega} q = 0\},$$

where  $H^1(\Omega) = \{\mathbf{v} \in L^2 : D^\alpha \mathbf{v} \in L^2(\Omega), \forall |\alpha| \leq 1\}$  is a Hilbert space and derive the classical variational formulation of the blood flow problem (1). To do that the system of equations (1) is multiplied by a pair of test functions  $(\mathbf{v}, q) \in (V, Q)$  for the velocity field and pressure and integrated over the domain  $\Omega$ . Moreover, we define the following bi- and trilinear forms

$$\begin{aligned} m : V \times V &\rightarrow \mathbb{R} & : m(\mathbf{u}, \mathbf{v}) &= \int_{\Omega} \rho \mathbf{u} \cdot \mathbf{v}, \\ c : V \times V \times V &\rightarrow \mathbb{R} & : c(\mathbf{u}, \mathbf{v}, \mathbf{w}) &= \int_{\Omega} \rho (\mathbf{u} \cdot \nabla \mathbf{v}) \cdot \mathbf{w}, \\ a : V \times V &\rightarrow \mathbb{R} & : a(\mathbf{u}, \mathbf{v}) &= \int_{\Omega} 2\mu(\dot{\gamma}) \mathbf{D}(\mathbf{u}) \mathbf{D}(\mathbf{v}), \\ b : V \times Q &\rightarrow \mathbb{R} & : b(\mathbf{u}, q) &= \int_{\Omega} q \operatorname{div} \mathbf{u}. \end{aligned}$$

Then, the weak formulation for the blood flow problem (1) reads as follows

Find the pair  $(\mathbf{u}, p) \in (V, Q)$  such that for all  $(\mathbf{v}, q) \in (V, Q)$  we have

$$\begin{aligned} m(\mathbf{u}_t, \mathbf{v}) + c(\mathbf{u}, \mathbf{u}, \mathbf{v}) + a(\mathbf{u}, \mathbf{v}) - b(p, \mathbf{v}) - b(\mathbf{u}, q) + \frac{1}{\epsilon^*} \int_{\Omega_{Clot}} \mathbf{u}\mathbf{v} \\ = - \int_{\partial\Omega} \frac{1}{\beta} (\mathbf{u} \cdot \boldsymbol{\tau}_1) (\mathbf{v} \cdot \boldsymbol{\tau}_1) - \int_{\partial\Omega} \frac{1}{\beta} (\mathbf{u} \cdot \boldsymbol{\tau}_2) (\mathbf{v} \cdot \boldsymbol{\tau}_2). \end{aligned} \quad (17)$$

Here, the last integral on the left hand side meant to model the blood clot. According to it the blood velocity is penalized in those computational nodes where fibrin has achieved its threshold. Parameter  $\epsilon^*$  is chosen as a very small number and we introduce a characteristic function  $H$  dependent on fibrin concentration, such

$$\int_{\Omega_{Clot}} \mathbf{u}\mathbf{v} = \int_{\Omega} (1 - H) \mathbf{u}\mathbf{v}.$$

Let the domain  $\Omega$  be approximated by  $\Omega_h = \bigcup_{k=1}^{n_t} \mathcal{T}_k$ , where  $\{\mathcal{T}_k\}_{k=1, \dots, n_t}$  is a family of tetrahedra. Problem (17) is approximated according to the Galerkin method [30, 41] also applying the penalty method [23]. Finally, the weak formulation reads as follows

Find the pair  $(\mathbf{u}_h^\epsilon, p_h^\epsilon) \in (V_h, \bar{Q}_h) \subset (V, Q)$  satisfying the following equations

$$\begin{aligned} m((\mathbf{u}_h^\epsilon)_t, \mathbf{v}_h) + c(\mathbf{u}_h^\epsilon, \mathbf{u}_h^\epsilon, \mathbf{v}_h) + a(\mathbf{u}_h^\epsilon, \mathbf{v}_h) - b(p_h^\epsilon, \mathbf{v}_h) - b(\mathbf{u}_h^\epsilon, q_h) \\ + \frac{1}{\epsilon^*} \int_{\Omega_{Clot}} \mathbf{u}_h^\epsilon \mathbf{v}_h^\epsilon \\ = - \int_{\partial\Omega} \frac{1}{\beta} (\mathbf{u}_h^\epsilon \cdot \boldsymbol{\tau}_1) (\mathbf{v}_h \cdot \boldsymbol{\tau}_1) - \int_{\partial\Omega} \frac{1}{\beta} (\mathbf{u}_h^\epsilon \cdot \boldsymbol{\tau}_2) (\mathbf{v}_h \cdot \boldsymbol{\tau}_2), \\ \forall (\mathbf{v}_h, q_h) \in (V_h, \bar{Q}_h); \end{aligned} \quad (18)$$

and

$$\operatorname{div} \mathbf{u}_h^\epsilon = \epsilon p_h^\epsilon,$$

where  $\epsilon$  is a very small number.

A classical Taylor-Hood element technique is adopted to approximate the velocity vector field  $\mathbf{u}$  and the pressure scalar function  $p$

$$\begin{aligned} V_h &:= \{\mathbf{v} \in H^1(\Omega)^2 \mid \forall K \in \mathcal{T}_h, v|_K \in P_2\} \text{ and} \\ Q_h &:= \{q \in H^1(\Omega) \mid \forall K \in \mathcal{T}_h, q|_K \in P_1\}. \end{aligned}$$

Time discretization of (18) is done by an implicit Euler scheme subdividing the time interval  $[t_{PP}, T]$  into a number of subintervals  $(t_n, t_{n+1})$ ,  $n = 0, \dots, N$ . To discretize the convective term a semi-implicit scheme is adopted. Finally, the following vector-matrix form is derived

$$\begin{aligned} M \frac{\mathbf{U}^{n+1} - \mathbf{U}^n}{\Delta t} + C(\mathbf{U}^n) \mathbf{U}^{n+1} + A \mathbf{U}^{n+1} + \mathbf{B}^T \mathbf{P}^{n+1} \\ + B \mathbf{U}^{n+1} + S \mathbf{U}^{n+1} + \frac{1}{\epsilon} H \mathbf{U}^{n+1} = \mathbf{0}, \end{aligned}$$

where the velocity and pressure are defined as  $\mathbf{U}(t) = \{u_1(t), \dots, u_M(t)\}^T$  and  $\mathbf{P}(t) = \{p_1(t), \dots, p_N(t)\}^T$  and the matrices arising from the bi- and trilinear forms are

$$\begin{aligned} M &= \{M_{ij}\}_{i,j}^M \quad \text{such that} \quad M_{ij} = m(\varphi_i, \varphi_j), \\ C(\mathbf{U}(t)) &= \{C_{ij}(\mathbf{U}(t))\}_{i,j,k}^M \quad \text{such that} \quad C_{ij}(\mathbf{U}(t)) = c \left( \sum_{k=1}^M u_k(t) \varphi_k, \varphi_i, \varphi_j \right), \\ A &= \{A_{ij}\}_{i,j}^M \quad \text{such that} \quad A_{ij} = a(\varphi_i, \varphi_j), \\ B &= \{B_{ik}\}_{i,k}^{M,N} \quad \text{such that} \quad B_{ik} = b(\varphi_i, \phi_k), \\ H &= \{H_{ij}\}_{i,j}^M \quad \text{such that} \quad H_{ij} = \frac{1}{\rho} m(\varphi_i, \varphi_j). \end{aligned}$$

Finally, the linear system with the penalization term takes the following form

$$\begin{pmatrix} \mathbf{E} & \mathbf{B}^T \\ \mathbf{B} & -\epsilon \mathbf{I} \end{pmatrix} \begin{pmatrix} \mathbf{U}^\epsilon \\ \mathbf{P}^\epsilon \end{pmatrix} = \begin{pmatrix} \mathbf{0} \\ \mathbf{0} \end{pmatrix},$$

where matrix  $\mathbf{E}$  is given by

$$\mathbf{E} = \frac{1}{\Delta t} \mathbf{M} + \mathbf{A} + \mathbf{C}(\mathbf{U}^n) + \mathbf{S} + \frac{1}{\epsilon} \mathbf{H}.$$

### 3.2. Biochemical problem

We proceed with the resolution of biochemical problem (2). We recall that platelets concentration should be updated at the beginning of each biochemical iteration.

The existence of simultaneous fast and slow reactions makes the system extremely complicated to be solved numerically. In particular, reactions that include different rate constants and greatly vary in magnitude, impose strong stability constraints on the time step size. Numerical difficulties also come from the large number of equations present in our model, from the stiffness of the reaction terms and from the advection-dominated nature of the problem (2).

To deal with all these potential causes of numerical instabilities we use a second order operator (Strang) splitting method [24, 25, 28, 45, 49] and split (2) into two simpler subproblems—the reaction and the advection-diffusion (AD) one [8]—that are solved sequentially on each time interval  $[t_n, t_{n+1}]$ .

$$\left\{ \begin{array}{l} \frac{\partial C^*}{\partial t} = R(C^*), \quad \text{on } (t_n, t_{n+\frac{1}{2}}), C^*(t_n) = C(t_n), \\ \frac{\partial C^{**}}{\partial t} = D\Delta C^{**} - \mathbf{u} \cdot \nabla C^{**}, \quad \text{on } (t_n, t_{n+1}), C^{**}(t_n) = C^*(t_{n+\frac{1}{2}}), \\ \frac{\partial C^{***}}{\partial t} = R(C^{***}), \quad \text{on } (t_{n+\frac{1}{2}}, t_{n+1}), C^{***}(t_{n+\frac{1}{2}}) = C^{**}(t_{n+1}), \end{array} \right. \quad (19)$$

with  $C(t_{n+1}) = C^{***}(t_{n+1})$ .

The sequential order of subproblems resolution is very important in this case and the stiff operator must always be the last one in the splitting scheme, i.e. in our case that is applied to the reaction part [45].

**3.2.1. Reaction subproblem.** We solve the first subproblem consisting of a system of 13 ordinary differential equations that describe the reaction chain of coagulation factors  $C$  on the time interval  $[t_n, t_{n+\frac{1}{2}}]$  and discretize them in time using the second order Trapezoidal rule

$$C_{n+\frac{1}{2}} = C_n + \frac{\Delta t}{2j} \left( R(t_n, C_n) + R\left(t_{n+\frac{1}{2}}, C_{n+\frac{1}{2}}\right) \right).$$

Here,  $j$  stands for the number of the subiterations within the reaction loop and  $R$  are the reaction terms given for each coagulation factor separately by (3)–(15). To solve the non-linear reaction terms the Newton-Raphson iteration is adopted

$$C_{n+\frac{1}{2}}^{(k+1)} = C_{n+\frac{1}{2}}^{(k)} - \frac{C_{n+\frac{1}{2}}^{(k)} - C_n - \frac{\Delta t}{2j} \left( R(t_n, C_n) + R\left(t_{n+\frac{1}{2}}, C_{n+\frac{1}{2}}^{(k)}\right) \right)}{I - \frac{\Delta t}{2j} J_n},$$

where  $J_n$  stands for an approximation to the Jacobian matrix

$$J_n = \frac{\partial R(t_n, C_n)}{\partial C}.$$

**3.2.2. Advection-diffusion subproblem.** We proceed with the advection-diffusion subproblem resolution on each time interval  $[t_n, t_{n+1}]$  and solve it using the Galerkin approximation.

First we define the finite element space for the test functions

$$W := \{w \in H^1(\Omega)^d : C|_{\partial\Omega} = g\},$$

and derive the weak formulation multiplying equation (2) by a test function  $w$  and integrating it over the domain  $\Omega$ .

After integration by parts and taking into account the fact that in our case the diffusion parameters  $D$  are constant and that  $\text{div } u = 0$  due to the fluid's incompressibility, we introduce the following bi- and trilinear forms

$$\begin{aligned} m : W \times W &\rightarrow \mathbb{R} & : & m(C, w) = \int_{\Omega} Cw, \\ c : V \times W \times W &\rightarrow \mathbb{R} & : & c(\mathbf{u}, C, w) = \int_{\Omega} (\mathbf{u} \cdot \nabla C) \cdot w, \\ a : W \times W &\rightarrow \mathbb{R} & : & a(C, w) = \int_{\Omega} \nabla C \nabla w \end{aligned}$$

and derive the weak formulation obtaining the semi-discrete approximation in space of the advection-diffusion problem.

Find  $C \in W$  such that for every  $w \in W$ :

$$\begin{aligned} m(C_t, w) + c(\mathbf{u}, C, w) + a(C, w) = & \quad (20) \\ - \int_{\partial\Omega_{slip} \cup \partial\Omega_{out}} \left( -D \frac{\partial C}{\partial \mathbf{n}} + uC \cdot \mathbf{n} \right) w + \int_{\partial\Omega_{in}} C^{blood} w. \end{aligned}$$

We introduce the same triangulation of the domain  $\Omega$  as in the case of the fluid problem (1)

$$\Omega_h = \bigcup_{k=1}^{n_t} \mathcal{T}_k,$$

where  $\{\mathcal{T}_k\}_{k=1, \dots, n_t}$  stands for a family of tetrahedrals.

The usual Galerkin approximation undergoes spurious oscillations in the case of the dominated convection flow. Therefore, in order to stabilize this behavior a Streamline-Upwind/Petrov-Galerkin stabilization technique (SUPG) [15, 26] is adopted to obtain a smooth solution. Thus, the final weak form is given as

Find  $C_h \in W_h \subset W$  such that for every  $w_h \in W_h \subset W$ :

$$\begin{aligned} m((C_h)_t, w_h) + c(\mathbf{u}_h, C_h, w_h) + a(C_h, w_h) & \quad (21) \\ + s_1(\mathbf{u}_h, C_h, w_h) + s_2(\mathbf{u}_h, C_h, w_h) + s_3(\mathbf{u}_h, C_h, w_h) = & \\ - \int_{\partial\Omega_{slip} \cup \partial\Omega_{out}} \left( -D \frac{\partial C_h}{\partial \mathbf{n}} + \mathbf{u}_h C_h \cdot \mathbf{n} \right) w_h + \int_{\partial\Omega_{in}} C^{in} w, & \end{aligned}$$

where the trilinear forms  $s_i$  are defined by

$$\begin{aligned} s_1 &= \sum_{K \in \mathcal{T}_h} \tau_K (C_h, \mathbf{u}_h \cdot \nabla w_h)_K, \\ s_2 &= \sum_{K \in \mathcal{T}_h} \tau_K (-D \Delta C_h, \mathbf{u}_h \cdot \nabla w_h)_K, \\ s_3 &= \sum_{K \in \mathcal{T}_h} \tau_K (\mathbf{u}_h \cdot \nabla C_h, \mathbf{u}_h \cdot \nabla w_h)_K. \end{aligned}$$

We obtain the following matrix-vector formulation

$$\mathbf{MC}_t(t) + \mathbf{CC}(t) + \mathbf{AC}(t) + \sum_{l=1}^3 \mathbf{S}_l \mathbf{C}(t) = \mathbf{0}, \quad (22)$$

where the vector of the concentrations is given by  $\mathbf{C}(t) = \{C_1(t), \dots, C_L(t)\}^T$  and mass, convection and stiffness matrices arising from the bi- and trilinear forms are given by

$$\begin{aligned} \mathbf{M} &= \{M_{ij}\}_{i,j}^L \quad \text{such that} \quad M_{ij} = m(\xi_i, \xi_j), \\ \mathbf{C} &= \{C_{ij}\}_{i,j,k}^L \quad \text{such that} \quad C_{ij} = c \left( \sum_{k=1}^L u_k(t) \xi_k, \xi_i, \xi_j \right), \\ \mathbf{A} &= \{A_{ij}\}_{i,j}^L \quad \text{such that} \quad A_{ij} = a(\xi_i, \xi_j), \\ \mathbf{S}_l &= \{S_{lij}\}_{i,j}^L \quad \text{such that} \quad S_{lij} = s_l \left( \sum_{k=1}^L u_k(t) \xi_k, \xi_i, \xi_j \right), l = 1, 2, 3. \end{aligned}$$

We proceed with the time discretization of problem (22) on the time interval  $[t_{PP}, T]$  that corresponds to the time period from the beginning of the propagation phase till the final clot dissolution. We choose the second-order backward differentiation formula (BDF) and on each time interval  $[t_n, t_{n+1}]$ ,  $n = 0, \dots, N$  we solve the problem

$$\mathbf{M} \frac{\mathbf{C}^{n+1} - \frac{4}{3}\mathbf{C}^{n+\frac{1}{2}} + \frac{1}{3}\mathbf{C}^n}{\Delta t} - \frac{2}{3} \left( \mathbf{C}\mathbf{C}^{n+1} + \mathbf{A}\mathbf{C}^{n+1} + \sum_{i=1}^3 \mathbf{S}_i \mathbf{C}^{n+1} \right) = \mathbf{0}.$$

Finally the solution of the second subproblem is given in the following form:

$$\mathbf{C}^{n+1} = \left( \frac{\mathbf{M}}{\Delta t} - \frac{2}{3} \left( \mathbf{A} + \mathbf{C} + \sum_{i=1}^3 \mathbf{S}_i \right) \right)^{-1} \frac{\mathbf{M}}{\Delta t} \left( \frac{4}{3}\mathbf{C}^{n+\frac{1}{2}} - \frac{1}{3}\mathbf{C}^n \right), \quad (23)$$

where  $\mathbf{C}^{n+\frac{1}{2}}$  is taken as the solution of the first reaction subproblem of the current iteration and  $\mathbf{C}^n$  is the solution obtained at the end of the previous iteration.

**3.2.3. Second reaction subproblem.** For the resolution of the third subproblem—reaction part on the time interval  $[t_{n+\frac{1}{2}}, t_{n+1}]$ , we apply the same technique as in case of the first subproblem

$$\mathbf{C}^{n+1} = \mathbf{C}^{n+\frac{1}{2}} + \frac{\Delta t}{2j} \left( R(t_{n+\frac{1}{2}}, \mathbf{C}_{n+\frac{1}{2}}) + R(t_{n+1}, \mathbf{C}_{n+1}) \right),$$

taking the value  $\mathbf{C}_{n+\frac{1}{2}}$  as a solution of the advection-diffusion problem (23).

The solution of the final subproblem will be the solution of the whole reaction-advection-diffusion problem on the time interval  $[t_n, t_{n+1}]$ . We proceed to the next iteration in the same manner.

## 4. Numerical results

Finally, we present the numerical results of the blood clot evolution within the blood flow during the propagation and fibrinolysis phases, Fig. 2.

We would like to draw the reader's attention to the fact that the action of convection on fibrin was reduced up to 10% of the local value of the blood velocity. This assumption is justified by the fact that the created fibrin molecules immediately polymerize making strong connections with each other, and therefore, the polymer fibrin stays more resistant to the blood flow. This simplification was also applied in the two-dimensional case for consistency, however, numerical tests have shown that in the case of mesh refinement it can be avoided.

### 4.1. Anticoagulant dominance case

The main goal is also to show the capacity of the blood coagulation model to predict different disorder cases. Therefore, three different tests have been considered: the cases of anticoagulant dominance, hypercoagulation and platelets deficiency<sup>13</sup>.

<sup>13</sup>To save the computational time these numerical tests were performed in 2D, however we note that all of them are possible in 3D, with no major problems.

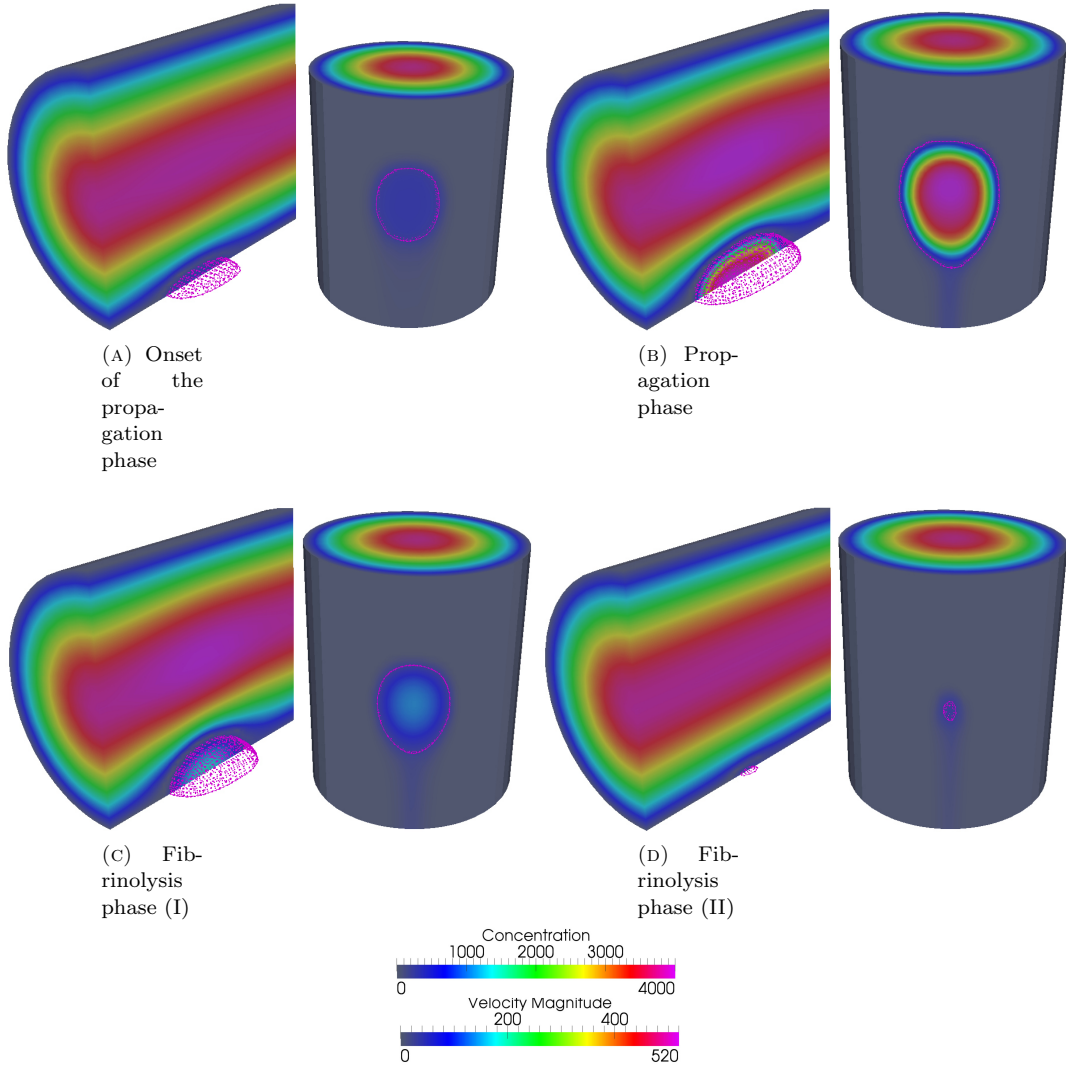


FIGURE 2. 3D simulations of the platelets-fibrin clot evolution.

As an example of anticoagulant dominance, the case of an increased ATIII concentration by 30% in blood is considered and compared to the normal blood.

The concentration plots for the main coagulation factors—fibrin, thrombin and prothrombinase—from the beginning of the propagation phase till the end of fibrinolysis (approximately 30 mins) also capturing their peak production during the propagation phase are shown in Fig. 3. It can be seen that the amount of the produced concentrations in this case is smaller comparing to the case of normal coagulation. Moreover, the clot at the peak of its evolution formed in the blood with the higher concentration of ATIII is also smaller comparing to the normal case as expected, Fig. 4.

#### 4.2. Hypercoagulation case

We refer to the opposite case of the one described in the previous section and study the possibility of the decrease of inhibitors in the blood. As an example the case of ATIII deficiency is considered, when the blood contains only 75% of the normal ATIII concentration. The concentration plots during the peak evolution and clot shape are shown in Figs. 5 and 6. As it was expected in the case of ATIII

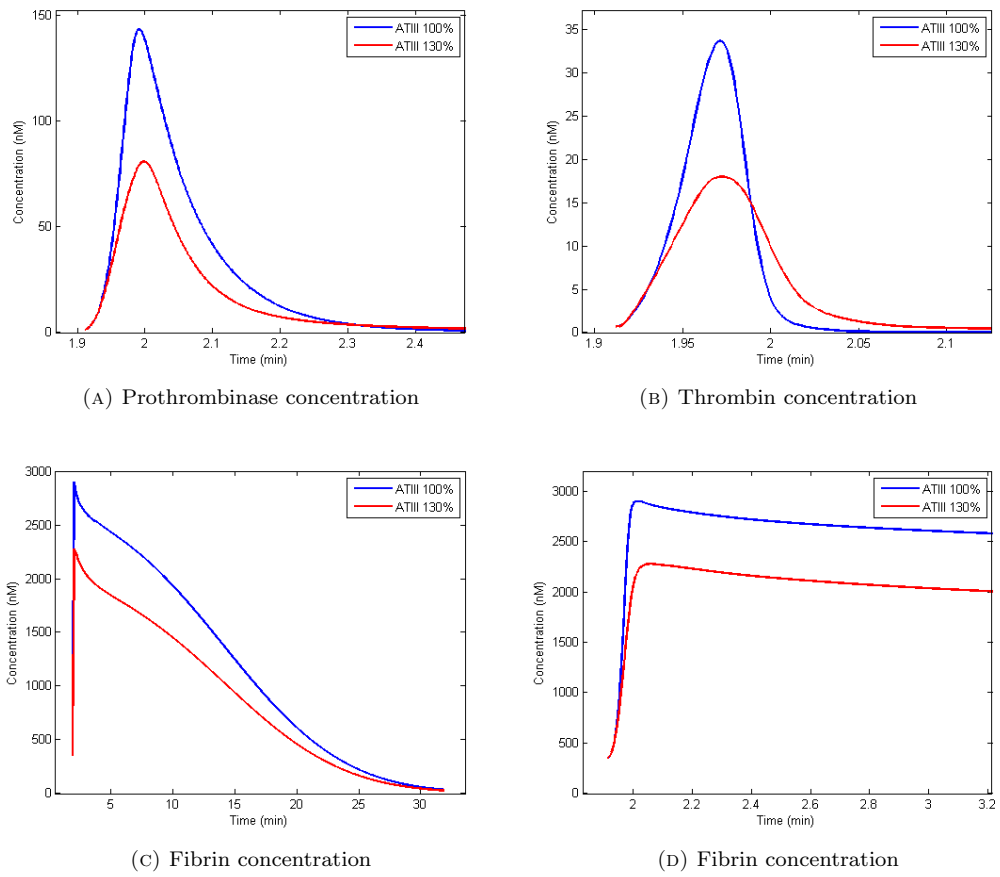


FIGURE 3. Evolution of the concentrations in the case of ATIII surplus.

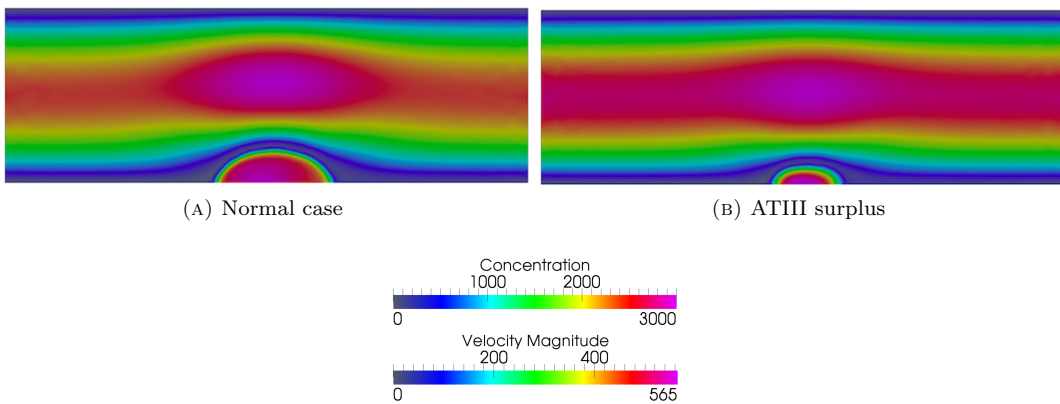


FIGURE 4. Blood clot size in the case of ATIII dominance at the peak of its formation.

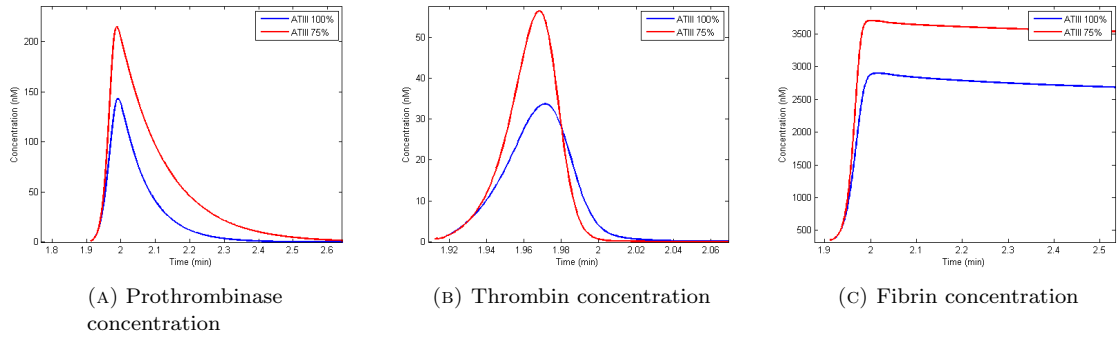


FIGURE 5. Evolution of the concentrations in the case of hypercoagulation.

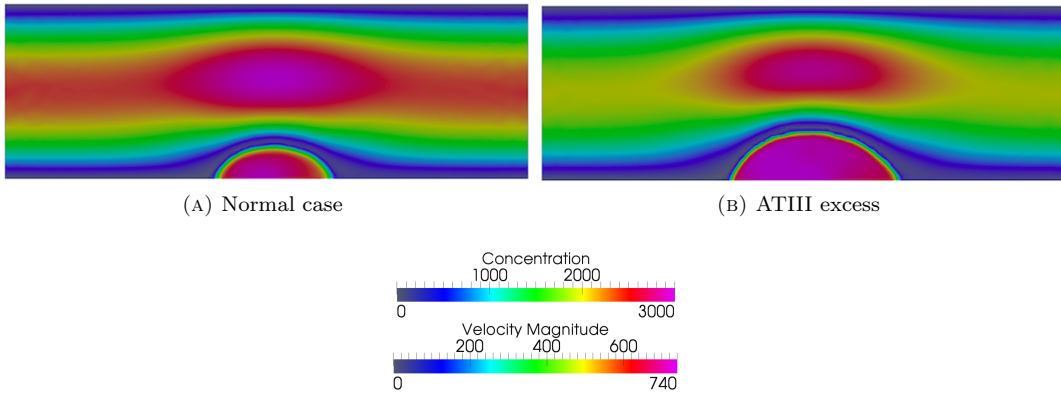


FIGURE 6. Blood clot size in the case of hypercoagulation at the peak of its formation.

deficiency the amount of produced thrombin and the size of the blood clot are much higher comparing to the normal case.

### 4.3. Platelets deficiency case

The next example is related to platelets deficiency in the clot formation process. As an example, we consider the amount of activated platelets supplied to the clotting region reduced by 10% and compare it with the normal case. The comparison in concentration production at the peak of the propagation phase and clot shape are shown in the Figs. 7 and 8.

The graphs show that in the case of the platelets deficiency there is a delay in thrombin production and additionally to that the produced amount of thrombin has also decreased resulting in a smaller and delayed fibrin production.

## 5. Conclusions

In this work we have carried out the numerical resolution of a mathematical model for the blood coagulation process incorporating the underlying biochemistry and the effect of the blood flow, including blood slip at the vessel wall. The model was formulated in [18] and the selection of the coefficients was made in [36] in a simplified geometrical context, using the differential system of [6] as a benchmark. Advantages of the present model are: a reduced set of equations, the intervention of activated platelets concentration, and the influence of blood slip in recruiting more platelets at the clotting site.

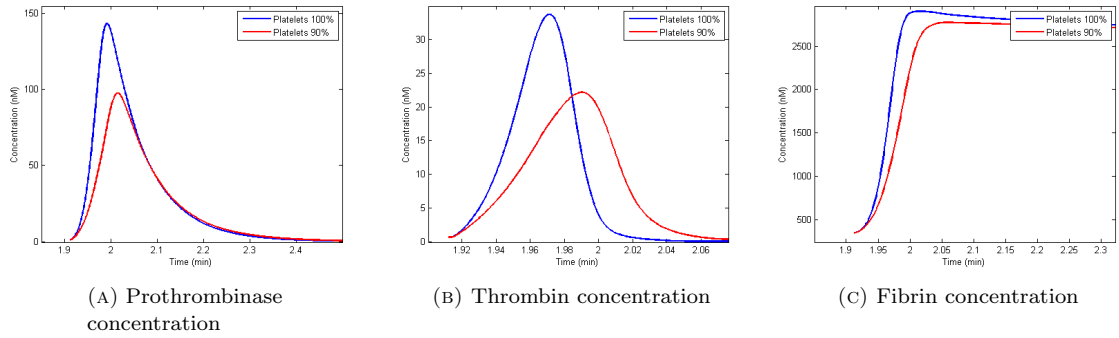


FIGURE 7. Evolution of prothrombin, thrombin and fibrin in the platelets deficiency case.

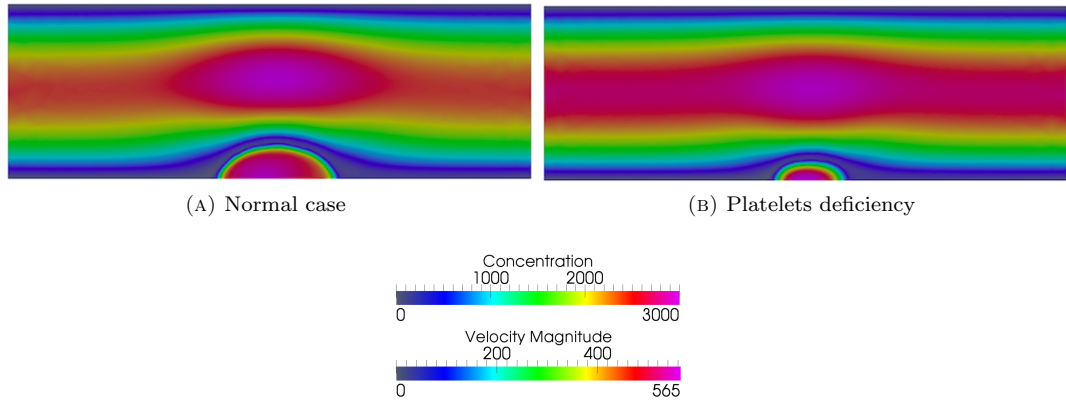


FIGURE 8. Blood clot size in the case of platelets deficiency at the peak of its formation.

The flow problem and the biochemical system were solved sequentially in such a way that at each time step the blood and clot domains were changing according to the fibrin concentration. In the computational nodes where fibrin concentration has reached a threshold value (defining the clot boundary) the blood velocity has been penalized making the clot resistant to the blood flow. Therefore, the biochemical components became affected by the blood flow only in those regions where fibrin concentration was below the threshold. The FEM was used for the space discretization of the blood coagulation model. The time discretization of the blood flow problem was done using the Euler implicit scheme and the nonlinear convective term was linearized using a semi-implicit scheme. The biochemical problem was solved using a second-order splitting method decomposing it into the reaction and advection-diffusion parts that were solved sequentially. The time discretization was done using second-order implicit schemes: trapezoidal rule for the reaction problem and second-order backward differentiation formula for the advection-diffusion one, to keep the splitting method error close to the second order. The linear systems arising from space and time discretization were solved numerically using the sparse and direct parallel solver MUMPS.

Major concerns in the numerical resolution were: the existence of numerical instabilities, loss of accuracy and a very large computational time when small time steps or a refined mesh have been used. Special techniques have been adopted to overcome most of these difficulties in order to obtain reliable results. Moreover, as a future work, the numerical resolution of the problem could be improved and the computational time could be reduced using a domain decomposition method.

The numerical results showed that the model allows to describe the coagulation process, including both the thrombin burst and clot dissolution, emphasizing the influence of particular features, like blood slip at the wall. The model is flexible enough to investigate e.g. the effects of abnormal values of antithrombin.

## Acknowledgments

This work was supported by Fundação para a Ciência e a Tecnologia (FCT) through the grant SFRH/BD/63334/2009 and the Center for Mathematics and its Applications of the Instituto Superior Técnico, University of Lisbon, in particular the project PHYSIOMATH (EXCL/MAT-NAN/0114/2012).

## References

- [1] M. Anand, Rajagopal, A mathematical model to describe the change in the constitutive character of blood due to platelet activation, *C. R. Mec.* **330**(8) (2002), 557–562.
- [2] M. Anand, K. Rajagopal and K.R. Rajagopal, A model incorporating some of the mechanical and biochemical factors underlying clot formation and dissolution in flowing blood, *Journal of Theoretical Medicine* **5**(3–4) (2003), 183–218.
- [3] M. Anand, K.R. Rajagopal, A shear-thinning viscoelastic fluid model for describing the flow of blood, *Int. J. Cardiovasc. Med. Sci.* **4**(2) (2004), 59–68.
- [4] M. Anand, K. Rajagopal, K.R. Rajagopal, A model for the formation and lysis of blood clots, *Pathophysiol. Haemost. Thromb.* **34**(2–3) (2005), 109–120.
- [5] M. Anand, K. Rajagopal, K.R. Rajagopal, A viscoelastic fluid model for describing the mechanics of a coarse ligated plasma clot, *Theor. Comput. Fluid Dyn.* **20**(4) (2006), 239–250.
- [6] M. Anand, K. Rajagopal and K.R. Rajagopal, A model for the formation, growth, and lysis of clots in quiescent plasma. A comparison between the effects of antithrombin III deficiency and protein C deficiency, *Journal of Theoretical Biology* **253** (2008), 725–738.
- [7] J.P. Antovic and M. Blombäck, *Essential guide to blood coagulation*, Blackwell Publishing Ltd, 2010.
- [8] S.H. Aydin and C. Çiftçi, The finite element method solution of variable diffusion coefficient convection-diffusion equations, *AIP Conf Proc* **1470** (2012), 228–231.
- [9] H.R. Baumgartner, The role of blood flow in platelet adhesion, fibrin deposition, and formation of mural thrombi, *Microvascular Research* **5** (1973), 167–179.
- [10] J.P. Bertram, C.A. Williams and E.B. Lavik, Synthetic platelets: Nanotechnology to halt bleeding, *Sci Transl Med.* **1**(11) (2009), 11-22.
- [11] I. Borsi, A. Farina, A. Fasano and K.R. Rajagopal, Modelling the combined chemical and mechanical action for blood clotting. In: *Nonlinear Phenomena with Energy Dissipation, Gakuto Internat Ser Math Sci Appl*, Gakkotosho, Tokyo, **29** (2008), 53–72.
- [12] A.M. Bruaset and A. Tveito, (eds.), Numerical solution of partial differential equations on parallel computers, *Lecture Notes in Computational Science and Engineering*, **51**, 2006. ISBN 978-3-540-29076-6.
- [13] S. Butenas, C. van't Veer and K.G. Mann, "Normal" thrombin generation, *Blood* **94**(7) (1999), 2169–2178.
- [14] S.H. Caldwell, M. Hoffman, T. Lisman, B.G. Macik, P.G. Northup, K.R. Reddy, A. Tripodi and A.J. Sanyal, Coagulation disorders and hemostasis in liver disease: pathophysiology and critical assessment of current management, *Hepatology* **44**(4) (2006), 1039–1046.
- [15] R. Codina, Finite element approximation of the convection-diffusion equation: Subgrid-scale spaces, local instabilities and anisotropic space-time discretizations, In: *BAIL 2010 - Boundary and Interior Layers, Computational and Asymptotic Methods Lecture Notes in Computational Science and Engineering* **81** (2011), 85–97.
- [16] A.T. Cohen, G. Agnelli, F.A. Anderson, J.I. Arcelus, D. Bergqvist, J.G. Brecht, I.A. Greer, J.A. Heit, J.L. Hutchinson, A.K. Kakkar, D. Mottier, E. Oger, M.-M. Samama, M. Spannagl, Venous thromboembolism (VTE) in Europe - The number of VTE events and associated morbidity and mortality, *textitThrombosis and Haemostasis* **98** (2007), 756–764

- [17] B. Dahlbäck, Blood coagulation and its regulation by anticoagulant pathways: genetic pathogenesis of bleeding and thrombotic diseases, *Journal of Internal Medicine* **257** (2005), 209–223.
- [18] A. Fasano, J. Pavlova and A. Sequeira, A synthetic model for blood coagulation including blood slip at vessel wall, *Clinical Hemorheology and Microcirculation* **51** (2012), 1–14.
- [19] A. Fasano, R. Santos and A. Sequeira, Blood coagulation: a puzzle for biologists, a maze for mathematicians. In *Modelling Physiological Flows*, D. Ambrosi, A. Quarteroni, G. Rozza (Editors), Springer Italia Chapt. 3, (2011) 44–77, DOI 10.1007/978-88-470-1935-53.
- [20] A.L. Fogelson and J.P. Keener, Toward an understanding of fibrin branching structure, *Phys Rev E Stat Nonlin Soft Matter Phys* **81**(5–1) (2010), 051922.
- [21] A.I. Fogelson and R.D. Guy, Immersed-boundary-type models of intravascular platelet aggregation, *Comput Appl. Mech. Engrg.* **197** (2008), 2087–2104.
- [22] B. Furie and B.C. Furie, Thrombus formation in vivo, *J Clin Invest* **115**(12) (2005), 3335–3362.
- [23] F. Hecht, New development in FreeFem++. *J. Numer. Math.* 20 (3–4) (2012), 251–265. 65Y15, <http://www.freefem.org>
- [24] W.H. Hundsdorfer, Numerical solution of advection-diffusion-reaction equations, *Lecture notes*, Thomas Stieltjes Institute, 1996.
- [25] T. Jahnke and C. Lubich, Error bounds for exponential operator splittings, *BIT*, **40**(4) (2000), 735–744.
- [26] V. John and J. Novo, Error analysis of the SUPG finite element discretization of evolutionary convection-diffusion-reaction equations, *SIAM J Numer Anal* **49**(3) (2011), 1149–1176.
- [27] B.W. Kernighan and D.M. Ritchie, *The C programming Language*, 2nd Edition, Prentice-Hall PTR, 1988. ISBN 0-13-110362-8.
- [28] R.I. McLachlan and G.R.W. Quispel, Splitting methods, *Acta Numerica* **11** (2002), 341–434.
- [29] D.E. LaCroix and M. Anand, A model for the formation, growth, and dissolution of clots in vitro. Effect of the intrinsic pathway on antithrombin III deficiency and protein C deficiency, *Int J Eng Sci Appl Math* **3**(1–4) (2011), 93–105.
- [30] M.G. Larson and F. Bengzon, The finite element method: theory, implementation, and practice, *Texts in Computational Science and Engineering*, Springer, **10**, 2010. ISBN 978-3-642-33287-6.
- [31] K. Leiderman and A.L. Fogelson, Grow with the flow: a spatial-temporal model of platelet deposition and blood coagulation under flow, *Mathematical Medicine and Biology* **28** (2011), 47–84.
- [32] P.M. Mannucci, Platelet/von Willebrand factor inhibitors to the rescue of ischemic stroke, *Arterioscler Thromb Vasc Biol* **30** (2010), 1882–1884.
- [33] T. Orfeo, M. Gissel, S. Butenas, A. Undas, K.E. Brummel-Ziedins and K.G. Mann, Anticoagulants and the propagation phase of thrombin generation, *PLoS ONE* **6**(11) (2011), e27852.
- [34] M.A. Panteleev, N.M. Ananyeva, N.J. Greko, F.I. Ataulakhanov and E.L. Saenko, Two subpopulations of thrombin-activated platelets differ in their binding of the components of the intrinsic factor X-activating complex, *J Thromb Haemost* **3** (2005), 2545–2553.
- [35] T.G. Papaioannou and C. Stefanadis, Vascular wall shear stress: basic principles and methods, *Hellenic J Cardiol* **46** (2005), 9–15.
- [36] J. Pavlova, A. Fasano, J. Janela and A. Sequeira, Numerical validation of a synthetic cell-based model of blood coagulation, *submitted*.
- [37] J. Pavlova, Mathematical modelling and numerical simulations of blood coagulation, PhD Thesis, Lisbon University, 2014.
- [38] I.V. Pivkin, P.D. Richardson and G. Karniadakis, Blood flow velocity effects and role of activation delay time on growth and form of platelet thrombi, *PNAS* **103**(46) (2006), 17164–17169.
- [39] W.H. Press, S.A. Teukolsky, W.T. Vetterling and B.P. Flannery, *Numerical Recipes 3rd Edition: The Art of Scientific Computing*, Cambridge University Press, New York, 2007. ISBN 978-0-521-88068-8.
- [40] M.J. Quinn, *Parallel Programming in C with MPI and OpenMP*, McGraw-Hill, New-York, 2004. ISBN 007-123265-6.
- [41] Ir.A. Segal, *Finite Element methods for the Incompressible Navier-Stokes Equations*, Delft University of Technology, Delft, 2012.

- [42] F. Shen, C.J. Kastrup, Y. Liu and R.F. Ismagilov, Threshold response of initiation of blood coagulation by tissue factor in patterned microfluidic capillaries is controlled by shear rate, *Arterioscler Thromb Vasc Biol* **28** (2008), 2035–2041.
- [43] A.M. Shibeko, S.S. Karamzin, A.A. Butylin, M.A. Panteleev and F.I. Ataullakhanov, The review of contemporary ideas about the influence of flow rate on blood clotting, *Biochemistry (Moscow) Supplement Series A: Membrane and Cell Biology* **4**(3) (2009), 388–394.
- [44] A.M. Shibeko, E.S. Lobanova, M.A. Panteleev and F.I. Ataullakhanov, Blood flow controls coagulation onset via the positive feedback of factor VII activation by factor Xa, *BMC Systems Biology* **4**(5) (2010), 1–12.
- [45] B. Sportisse, An analysis of operator splitting techniques in the stiff case, *Journal of Computational Physics* **161** (2000), 140–168.
- [46] M.V. Ovanosov, N.M. Ananyeva, M.A. Panteleev, F.I. Ataullakhanov and E.L. Saenko, Initiation and propagation of coagulation from tissue factor-bearing cell monolayers to plasma: initiator cells do not regulate spatial growth rate, *J Thromb Haemost* **3** (2005), 321–331.
- [47] B.C.H. Verbiest, Thrombus formation in aneurysms: an experimental study, *Master Thesis*, Eindhoven University of Technology, 2008.
- [48] F.F. Weller, A free boundary problem modeling thrombus growth: Model development and numerical simulation using the level set method, *J Math Biol* **61**(6) (2010), 805–818.
- [49] S. Zhao, J. Ovadia, X. Liu, Y.-T. Zhang and Q. Nie, Operator splitting implicit integration factor methods for stiff reaction-diffusion-advection systems, *J Comput Phys* **230**(15) (2011), 5996–6009.

Jevgenija Pavlova

CEMAT, IST, Universidade de Lisboa, Portugal

e-mail: [jevgenija.pavlova@gmail.com](mailto:jevgenija.pavlova@gmail.com)

Antonio Fasano

Professor Emeritus, Dipartimento di Matematica, "U. Dini", Università degli studi di Firenze, Italy

Scientific Manager at FIAB SpA, Firenze, Italy

Istituto di Analisi dei Sistemi ed Informatica (IASI) Antonio Ruberti, CNR, Italy

e-mail: [fasano@math.unifi.it](mailto:fasano@math.unifi.it)

Adélia Sequeira

CEMAT, IST, Universidade de Lisboa, Portugal

Departamento de Matemática, IST, Universidade de Lisboa, Portugal

e-mail: [adelia.sequeira@math.ist.utl.pt](mailto:adelia.sequeira@math.ist.utl.pt)